

Second-order fluctuation theory and time autocorrelation function for currents

Roman Belousov*

The Rockefeller University, New York 10065, USA

E.G.D. Cohen†

The Rockefeller University, New York 10065, USA and

Department of Physics and Astronomy, The University of Iowa, Iowa City, Iowa 52242, USA

(Dated: October 17, 2016)

By using recent developments for the Langevin dynamics of spatially asymmetric systems, we routinely generalize the Onsager-Machlup fluctuation theory of the second order in time. In this form, it becomes applicable to fluctuating variables, including hydrodynamic currents, in equilibrium as well as nonequilibrium steady states. From the solution of the obtained stochastic equations we derive an analytical expression for the time autocorrelation function of a general fluctuating quantity. This theoretical result is then tested in a study of a shear flow by molecular dynamics simulations. The proposed form of the time autocorrelation function yields an excellent fit to our computational data for both equilibrium and nonequilibrium steady states. Unlike the analogous result of the first-order Onsager-Machlup theory, our expression correctly describes the short-time correlations. Its utility is demonstrated in an application of the Green-Kubo formula for the transport coefficient. Curiously, the normalized time autocorrelation function for the shear flow, which only depends on the deterministic part of the fluctuation dynamics, appears independent of the external shear force in the linear nonequilibrium regime.

I. INTRODUCTION

The stochastic theory of fluctuations for physical systems in equilibrium, due to Onsager and Machlup, was originally presented in two forms, Refs. [1] and [2], respectively, which were published together in the same journal issue. One of these papers [1] describes a model based on the Langevin differential equation of the first order in time, while the other [2] was concerned with its extension to the second order in time. This latter model received relatively little attention compared to the first-order theory, which was much broader disseminated and is now included in classic and modern text books on Statistical Physics, e.g., Refs. [3, Chapter XII] or [4, Chapter 2].

The first-order fluctuation theory was generalized also to nonequilibrium steady states, e.g., Refs. [5–8]. The principle argument, on which Onsager and Machlup mainly relied in their papers, was the time reversibility. The recent developments [8–11], however, suggest to focus on the spatial symmetry of fluctuating physical systems. This allows to apply the Onsager-Machlup theory, originally restricted to physical quantities invariant under the time reversal [1, 2], also to currents.

According to the first-order Langevin dynamics, a time autocorrelation function $C_\alpha(t)$ of a fluctuating quantity $\alpha(t)$ is a decaying exponential [3, Chapter XII]:

$$C_\alpha(t) \propto \exp(-\text{const } |t|). \quad (1)$$

This analytical result agrees asymptotically with the long-time behavior of the correlations, found in experi-

ments and computer simulations of classical physical systems [4, Chapter 2]. Nonetheless, the first-order theory describes *inaccurately* correlations at short times, because the time derivative of Eq. (1) is discontinuous at $t = 0$, whereas one observes a smooth behavior with $\dot{C}_\alpha(0) = 0$ [4, Chapter 2].

This failure of the first-order theory to describe correlations at short times can be attributed to one of its underlying assumptions. Without loss of generality, consider, for instance, the fluctuations of an equilibrium system described by the ensemble averages $\langle \alpha(t) \rangle = 0$, $\langle \dot{\alpha}(t) \rangle = 0$, cf. Ref. [1]. Suppose, this system spontaneously fluctuates from an initial *complete* [3, Chapter XII] equilibrium state $\alpha(0) = 0$, $\dot{\alpha}(0) = 0$ to another state with $\alpha(t > 0) = \alpha_0 \neq 0$, $\dot{\alpha}(t > 0) \neq 0$. The first-order fluctuation theory regards $\dot{\alpha}(t)$ merely as a function¹ $\dot{\alpha}[\alpha(t)]$, i.e. entirely determined by $\alpha(t)$. Physically, this assumption implies, that the relaxation time from a general transient state α_0 , $\dot{\alpha} \neq \dot{\alpha}[\alpha_0]$ to the *incomplete equilibrium* state α_0 , $\dot{\alpha}[\alpha_0]$ is neglected, cf. [3, Chapter XII]. Therefore, the described *quasistationary* approach [3, Chapter XII] does not allow to consider the fluctuation dynamics at arbitrarily short time scales.

The second-order theory of Onsager and Machlup goes beyond the quasistationary approach, by using two independent variables $\alpha(t)$ and $\dot{\alpha}(t)$ to specify completely a system state. In the corresponding differential equation, which will be discussed shortly, a change of state $\alpha(t)$, $\dot{\alpha}(t)$ affects only the second derivative $\ddot{\alpha}(t)$. The fluctuation dynamics then becomes inertial and is capable of describing transient states, which were ignored in

* belousov.roman@gmail.com

† egdc@mail.rockefeller.edu

¹ One can formally define $\dot{\alpha}[\alpha(t)]$ by using a conditional ensemble average of $\dot{\alpha}(t)$ at a fixed value $\alpha(t)$, cf. [12].

the first-order theory. One should, therefore, expect that the second-order theory is applicable to even smaller time scales, than those accessible to the quasistationary approach.

In this paper the original second-order theory of Onsager and Machlup [2] is first generalized, as suggested in Ref. [8]. In this new form it becomes, in principle, applicable to both equilibrium and nonequilibrium steady-state systems. In Sec. II we solve the extended Langevin equation, thus obtained, for $\alpha(t)$ and $\dot{\alpha}(t)$ and then derive an analytical expression for the time autocorrelation function $C_\alpha(t)$, which is analogous to Eq. (1). Finally, the usefulness of these theoretical results is demonstrated in an applied study of shear flow correlations by means of computer simulations in Sec. III.

The time autocorrelation function, which follows from the second-order fluctuation theory, turns out to describe very accurately the results of our computer simulations and has the following form:

$$C_\alpha(t) \propto \exp\left(-\frac{a|t|}{2}\right) \left[\cosh\left(\frac{d|t|}{2}\right) + \frac{a}{d} \sinh\left(\frac{d|t|}{2}\right) \right], \quad (2)$$

where a and d are constants to be yet specified in Sec. II. Agreement of Eq. (2) with our computational data is observed not only for the long-time behavior, which remains exponential in character, but also for the short times. In particular, the time derivative of Eq. (2) is continuous at $t = 0$ with the expected value $\dot{C}_\alpha(0) = 0$. This improvement over the quasistationary approach, as discussed earlier, can be explained by the finer timescale resolution of the second-order fluctuation theory.

In Sec. III we demonstrate, by using our equilibrium simulations, one practical application of the analytical form, Eq. (2), for the current autocorrelation function. Namely, we evaluate its time integral in a Green-Kubo formula for the shear viscosity coefficient [13, Chapter 7]. In principle, this estimation method of the transport coefficient is more accurate than the usually employed procedure of numerical integration, as will be discussed.

Our computations show, that the parameters of the normalized current autocorrelation function are effectively independent of the external shear rate in the linear nonequilibrium regime. Their values agree with the ones found from our equilibrium simulations. This is consistent with the fact, that the shear viscosity, which is constant in the linear nonequilibrium regime, is related to the parameters of the normalized current autocorrelation function, see Sec. III.

II. THEORY

The linear Langevin equation of second order in time, proposed by Onsager and Machlup [2] for a fluctuating quantity $\alpha(t)$, can be expressed in the following general

form:

$$\frac{d^2\alpha(t)}{dt^2} + a\frac{d\alpha(t)}{dt} + b^2\alpha(t) = \epsilon(t), \quad (3)$$

where $a > 0$ and $b > 0$ are constants, while $\epsilon(t)$ is a random noise.

The left hand side (LHS) of Eq. (3) is analogous to the damped harmonic oscillator. As it also will become clear from the solution of this equation later in this section, the parameter a is a friction-like coefficient, which ensures an exponential relaxation to the macroscopically observable steady state $\langle\alpha(t)\rangle$ with $\langle\dot{\alpha}(t)\rangle = 0$, as well as a decay of correlations at long times. The potential-like term, proportional to b^2 , determines the resistance of the system to spontaneous fluctuations and external forces, both due to the right hand side (RHS) of Eq. (3). The constant b , which is analogous to the frequency of the harmonic oscillator, also affects the autocorrelation function at short times.

In the original theory of Onsager and Machlup for equilibrium systems, the stochastic part of Eq. (3), i.e. its RHS, which represents irregular spontaneous fluctuating dynamics due to the ignored degrees of freedom, was assumed Gaussian. Several generalization of $\epsilon(t)$ were recently announced [6–8] for the nonequilibrium states, in order to incorporate the action of an external force. Although in Appendices A and B we will treat a more general case, in this section we follow Ref. [8], by considering a non-Gaussian random noise of the form:

$$\epsilon(t) = AdW(t)/dt + BdE(t/\tau)/dt, \quad (4)$$

where $A > 0$ and $B \geq 0$ are constants, $dW(t)$ and $dE(t/\tau)$ are, respectively, white noise and exponential noise with a timescale τ , see Ref. [8].

In Equation (4) [8], the constant A is proportional to the system's temperature, while the ratio B/τ is the average value of an external nonequilibrium force. When $B = 0$, Eq. (3) naturally reduces to the equilibrium case with the Gaussian random noise, considered by Onsager and Machlup in Ref. [2]. The noise terms are defined as stochastic differentials of two random processes: i) the Gaussian process $W(t)$ with a zero mean and a unit variance, and ii) the Gamma process $E(t/\tau)$ with a timescale τ and a unit intensity.

In a steady-state the mean values of the time derivatives $\langle\dot{\alpha}(t)\rangle$ and $\langle\ddot{\alpha}(t)\rangle$ must vanish by definition. Therefore by taking the appropriate ensemble average on both sides of Eq. (3), one can read off immediately the macroscopic behavior of $\alpha(t)$, cf. Ref. [8]:

$$b^2\langle\alpha(t)\rangle = B/\tau, \quad (5)$$

which implies that for the equilibrium case one has $\langle\alpha(t)\rangle = 0$, while in the nonequilibrium steady-state the parameter b^2 determines the system's response to an external force $\langle\alpha(t)\rangle = B/(\tau b^2)$.

A formal solution of Eq. (3) for a general stochastic term $\epsilon(t)$ can be found in Ref. [14, Sec. II.3]. For that,

in principle, one must consider three cases of a discriminant $d^2 = a^2 - 4b^2$: i) a periodic solution $d^2 < 0$, ii) an aperiodic solution $d^2 = 0$, iii) and a nonperiodic solution $d^2 > 0$. In this paper we consider only the last one², because it is applied later in Sec. III to our simulations. Below we cite, in a more compact form, the nonperiodic

solution of Eq. (3) from Ref. [14, Sec. II.3]:

$$\alpha(t) - \alpha(0)c(t) + \dot{\alpha}(0)\dot{c}(t)/b^2 = \int_0^t ds \phi(t-s)\epsilon(s) \quad (6)$$

$$\dot{\alpha}(t) - \alpha(0)\dot{c}(t) + \dot{\alpha}(0)\ddot{c}(t)/b^2 = \int_0^t ds \dot{\phi}(t-s)\epsilon(s), \quad (7)$$

where

$$c(t) = \exp\left(-\frac{at}{2}\right) \left[\cosh\left(\frac{\sqrt{a^2 - 4b^2}}{2}t\right) + \frac{a}{\sqrt{a^2 - 4b^2}} \sinh\left(\frac{\sqrt{a^2 - 4b^2}}{2}t\right) \right] \quad (8)$$

$$\phi(t) = (a^2 - 4b^2)^{-1/2} \left[\exp\left(\frac{-a + \sqrt{a^2 - 4b^2}}{2}t\right) - \exp\left(\frac{-a - \sqrt{a^2 - 4b^2}}{2}t\right) \right]. \quad (9)$$

The problem, which remains to deal with in this paper, is to characterize the probability distribution of the random variables, given by the right hand sides of Eqs. (6 and 7). For the stochastic noise of the form Eq. (4), the probability density of these variables apparently can not be expressed in terms of elementary functions. Nonetheless a method, already shown in Ref. [8], allows to derive an integral representation of their cumulant-generating functions³ and, therefore, to compute analytically their statistical properties.

In Appendix A the cumulant-generating function of $\alpha(t)$ is obtained, as described just above. However, while discussing the time autocorrelation function $C_\alpha(t)$, we are mainly concerned with the steady-state (SS) solution of Eq. (3):

$$\alpha_{\text{SS}} = \lim_{t \rightarrow \infty} \alpha(t),$$

cumulants of which are also calculated in Appendix A. Indeed, the time autocorrelation function can be written as:

$$C_\alpha(t) = \langle \alpha(0)\alpha(t) \rangle - \langle \alpha^2(t) \rangle = \kappa_2(\alpha_{\text{SS}})c_\alpha(t), \quad (10)$$

where $\kappa_2(\alpha_{\text{SS}})$ is the second cumulant of α_{SS} or, in other words, its variance, and $c_\alpha(t)$ is the normalized time autocorrelation function, which corresponds to the Pearson correlation coefficient in the statistical terminology.

By inspecting Eq. (6), one can already see that the time-dependent solution $\alpha(t)$ contains a memory of its initial state $\alpha(0)$ and $\dot{\alpha}(0)$. With time this deterministic contribution is vanishing, so that the stochastic part due to the RHS of the equation, becomes progressively more

dominant. How quickly $\alpha(t)$ is forgetting its initial value $\alpha(0)$ is controlled by the function $c(t)$. This observation suggests, that $c(t)$ is related to the time autocorrelation function of $\alpha(t)$. In fact, in Appendix B we prove, that $c(t)$ is nothing else but its correlation coefficient:

$$c_\alpha(t) = c(t). \quad (11)$$

Equation (2) follows from the above one due to the time-reversal symmetry of the autocorrelations, with $d = \sqrt{a^2 - 4b^2}$.

Note, that the stochastic part of the second-order Langevin equation determines only the coefficient of proportionality $\kappa_2(\alpha_{\text{SS}})$ between $C_\alpha(t)$ and $c_\alpha(t)$ in Eq. (10). The normalized autocorrelation function, cf. Eqs. (8 and 11), depends only on the constant parameters of the deterministic terms in Eq. (3), namely a and b . This comes, perhaps, without a surprise, because the correlation is a measure of mutual deterministic dependence between quantities, $\alpha(t)$ and $\alpha(0)$ in this case. The stochastic term merely erases the connection between them, so that α_{SS} turns into a completely random variable. Drawn from this, another conclusion is that the analytical expression of the normalized autocorrelation function is the same for equilibrium and nonequilibrium cases, since they differ only by the stochastic part of Eq. (3).

III. SIMULATIONS

In this section we apply the theory, described in Sec. II, to study time autocorrelations of a shear flow by means of molecular dynamics simulations. Details of our computational model can be found in Appendix C. Here we just mention, that we consider a thermostatted Weeks-Chandler-Andersen (WCA) fluid [15] in three dimensions, with a constant shear rate γ maintained by the Lees-Edwards periodic boundary conditions [16, Chapter 6]. All results are reported in reduced units, cf. Appendix C.

² A simple prescription, how to obtain the periodic and aperiodic solutions of Eq. (3), can be found in Ref. [14, Sec. II.3].

³ A cumulant-generating function of a random variable is the Laplace transform of its probability density.

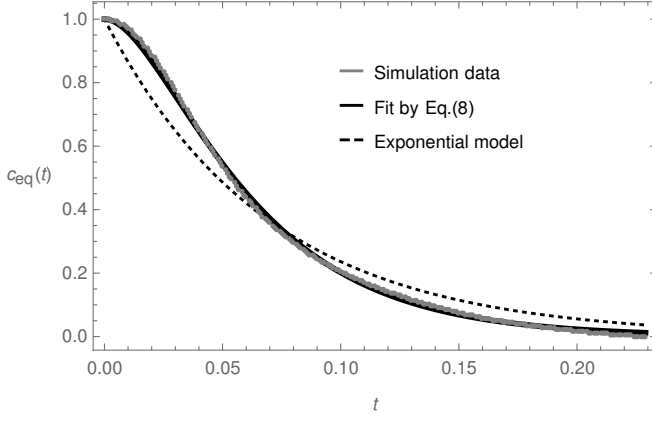


FIG. 1. Normalized time autocorrelation function $c_{\text{eq}}(t)$ of shear flow fluctuations in equilibrium: comparison of the molecular dynamics simulation data with their fits by analytical models: i) Eq. (8), proposed in this paper, ii) the exponential model of the first-order fluctuation theory Eq. (1).

The off-diagonal components of the pressure tensor P_{xy} , P_{yz} and P_{zx} are the three fluctuating observables, which we measure. They represent the transverse currents of the linear momentum, each obeying separately Eq. (3) by assumption. In our simulations of nonequilibrium steady-states, the external shear force $\gamma > 0$ causes an average shear flow $\langle P_{xy} \rangle < 0$, so that

$$\langle P_{xy} \rangle = -\eta\gamma, \quad (12)$$

where the transport coefficient η is the shear viscosity.

Let us begin, however, with the equilibrium simulations, i.e. $\gamma = 0$. In the absence of an external force, due to symmetry considerations, the statistical properties of $P_{xy}(t)$, $P_{yz}(t)$ and $P_{zx}(t)$ coincide. In particular, their equilibrium time autocorrelation functions are equal, respectively, $C_{xy}(t) = C_{yz}(t) = C_{zx}(t) = C_{\text{eq}}(t)$. This allows us to exploit more efficiently the statistics of measurements sample $\{P_{xy}(t_i), P_{yz}(t_i), P_{zx}(t_i)\}_{i=0..n-1}$ ($t_0 = 0$) of a given size n , as follows:

$$C_{\text{eq}}(t_i) = [C_{xy}(t_i) + C_{yz}(t_i) + C_{zx}(t_i)]/3 \quad (13)$$

$$C_{xy}(t_i) \approx \frac{1}{n-i} \sum_{j=0}^{n-i-1} P_{xy}(t_j)P_{xy}(t_{j+i}), \quad (14)$$

and similarly for C_{yz} and C_{zx} . The corresponding equilibrium normalized time autocorrelation function is

$$c_{\text{eq}}(t) = C_{\text{eq}}(t)/\kappa_2, \quad (15)$$

where κ_2 is the variance of the shear flow fluctuations in equilibrium, which is identical for P_{xy} , P_{yz} and P_{zx} . For a fixed n , the statistical uncertainty of resulting $C_{xy}(t_i)$ is growing with i , since the number of terms $n-i$ in Eq. (14) is then decreasing. Therefore we restrict the maximum considered time of correlations t_{max} by the widely ac-

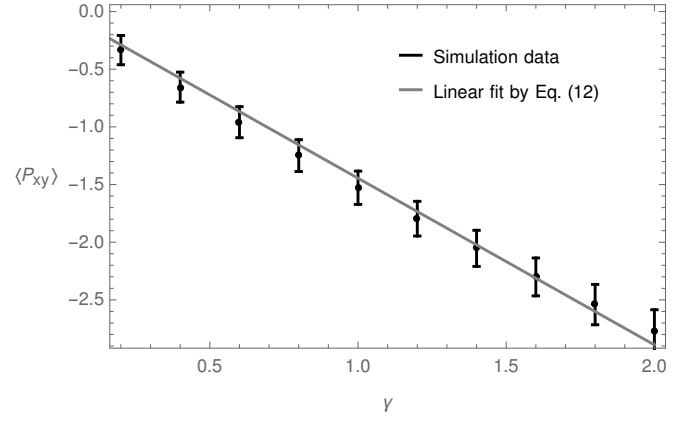


FIG. 2. Average current $\langle P_{xy} \rangle$, as a function of the externally applied shear rate γ , for our nonequilibrium steady-state simulations. The error bars are given by three standard deviations. A shear thinning, which corresponds to a decrease of the viscosity with γ , commonly observed for the WCA fluid, is statistically insignificant and negligible in the given hydrodynamic regime. Therefore the linear constitutive relation Eq. (12), with a constant viscosity η , renders a very good fit to simulation data.

cepted rule of “first zero”, due to Ref. [17].⁴

In Fig. 1 the normalized time autocorrelation function of the shear flow fluctuations, observed in our equilibrium simulations, is compared with its least-squares fit by Eq. (8). Our analytical model is in excellent agreement with the simulation data, including the region of short times. The exponential model, Eq. (1), which is also illustrated in Fig. 1 for comparison, demonstrates the failure of the first order fluctuation theory for $t \rightarrow 0$, discussed in Sec. I.

Provided that the shear viscosity in Eq. (12) is independent of γ , the equilibrium simulations allow to compute its value, η , via the Green-Kubo formula [16, Chapter 6]:

$$\eta = \frac{V}{k_B T} \int_0^\infty ds C_{\text{eq}}(t), \quad (16)$$

which together with Eqs. (8, 10, and 11) yields

$$\eta = \frac{a\kappa_2 V}{k_B T b^2}. \quad (17)$$

Equation (17) offers an alternative for a numerical approximation of the integral in Eq. (16) by a discrete sum:

$$\eta = \frac{V\Delta t}{k_B T} \sum_{i=0}^{t_{\text{max}}/\Delta t} C_{\text{eq}}(t_i), \quad (18)$$

⁴ The maximum time t_i does not exceed the first zero of the time autocorrelation function, i.e. $t_{\text{max}} < \inf\{t : C_{\text{eq}}(t_i) = 0\}$.

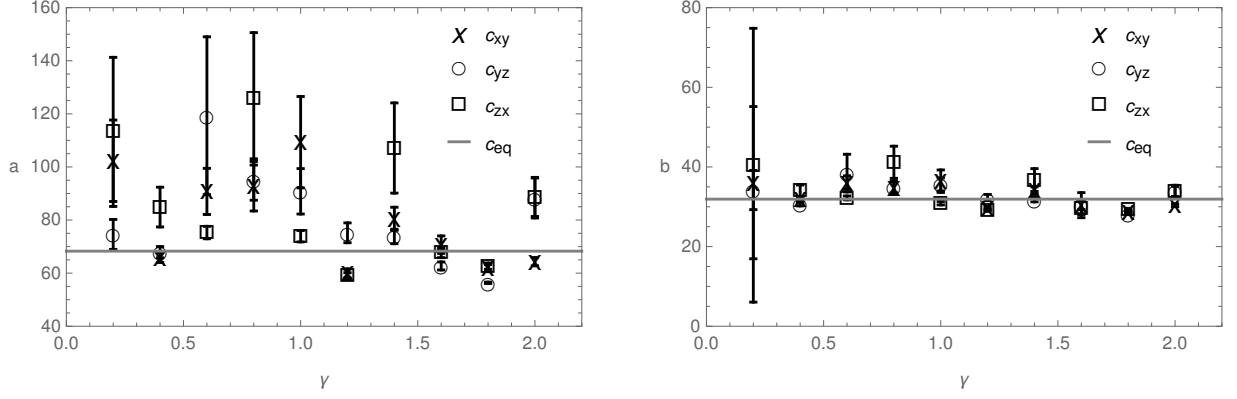


FIG. 3. Fitting parameters a and b of Eq. (8) for normalized time autocorrelation functions at various shear rates in our nonequilibrium steady-state simulations. Values of the parameters for equilibrium simulations are drawn as solid horizontal lines for comparison. Error bars are given by three standard deviations.

where Δt is the time step between successive measurements.

Indeed, our nonequilibrium simulations show, that the linear regime of constant viscosity spans a wide range of shear rates $\gamma \in (0, 2.0]$, as demonstrated by Fig. 2. Table I presents estimations of the shear viscosity, computed by various methods from our simulation data. All results are in very good agreement with each other. Equation (18), though, has a larger statistical uncertainty than Eq. (17), because the latter interpolates the behavior of the time autocorrelation function at successive time instants and, therefore, exploits more efficiently the simulation data. This inference may become even more important, if the time step Δt is larger than in our study or the number of measurements n is less.

Now we turn our attention to the time autocorrelations of shear currents in nonequilibrium steady states. Since the external force γ introduces a preferred spatial direction, the symmetry argument, which we used for Eq. (13), does not apply in this case. Therefore the nonequilibrium time autocorrelation functions $C_{xy}(t|\gamma)$, $C_{yz}(t|\gamma)$ and $C_{zx}(t|\gamma)$ should be considered separately:

$$C_{xy}(t_i|\gamma) = \kappa_2(P_{xy})c_{xy}(t_i|\gamma) \approx \frac{1}{n-i} \sum_{j=0}^{n-i-1} [P_{xy}(t_j)P_{xy}(t_{j+i}) - \langle P_{xy} \rangle^2] \Big|_{\gamma}, \quad (19)$$

TABLE I. Shear viscosity estimations, computed by various methods from simulation data.

Method	Shear viscosity (η)
Nonequilibrium simulations, Eq. (12)	1.445 ± 0.020
Green-Kubo formula, Eq. (17)	1.437 ± 0.095
Green-Kubo formula, Eq. (18)	1.44 ± 0.34

and similarly for $C_{yz}(t, \gamma)$ and $C_{zx}(t, \gamma)$, where $c_{xy}(t|\gamma)$ etc. stand for the normalized time autocorrelation functions.

Quite unexpectedly, we found that the parameters of our analytical model for the normalized autocorrelation functions did not exhibit any notable dependence on the shear rate. By inspecting Fig. 3, which presents results of fitting Eq. (8) to the simulation data, one observes no particular difference in the behavior of the parameters a and b between the three autocorrelation functions of interest. A remarkable aspect of these plots is that the points with smaller error bars are all close to the solid horizontal lines, which represent the values of a and b for the equilibrium function $c_{eq}(t)$. The large uncertainties of the data, which occur in the upper part of the graph, suggest that the statistical errors are biased and cause overestimation of the fitting parameters. This tendency can be explained by the errors of calculated values $c_{xy}(t_i)$, which are non-identically distributed and biased, see [18, Sec. 8.14]. Since no clearly visible trend is observed in Fig. 3 and the smaller errors of the estimations are close to the solid lines, we conclude that a and b are practically independent of the shear rate.

The above observations suggest to use the following averaging procedure for the normalized autocorrelation function of the nonequilibrium steady-state, independently of the shear rate:

$$c_{ne}(t_i) = \frac{1}{3} \left[\frac{C_{xy}(t_i)}{\kappa_2(P_{xy})} + \frac{C_{yz}(t_i)}{\kappa_2(P_{yz})} + \frac{C_{zx}(t_i)}{\kappa_2(P_{zx})} \right]. \quad (20)$$

Although Eq. (20) is somewhat similar to Eq. (13), the statistical uncertainty of the latter is much smaller for several reasons. First, the equilibrium autocorrelations are calculated by taking into account explicitly, that the average current vanishes $\langle P_{xy} \rangle = 0$, cf. Eqs. (14 and 19), while in the nonequilibrium case one uses the same measurements to evaluate $\langle P_{xy} \rangle$ and then Eq. (19). Second, measurements of P_{xy} , P_{yz} and P_{zx} are merged to com-

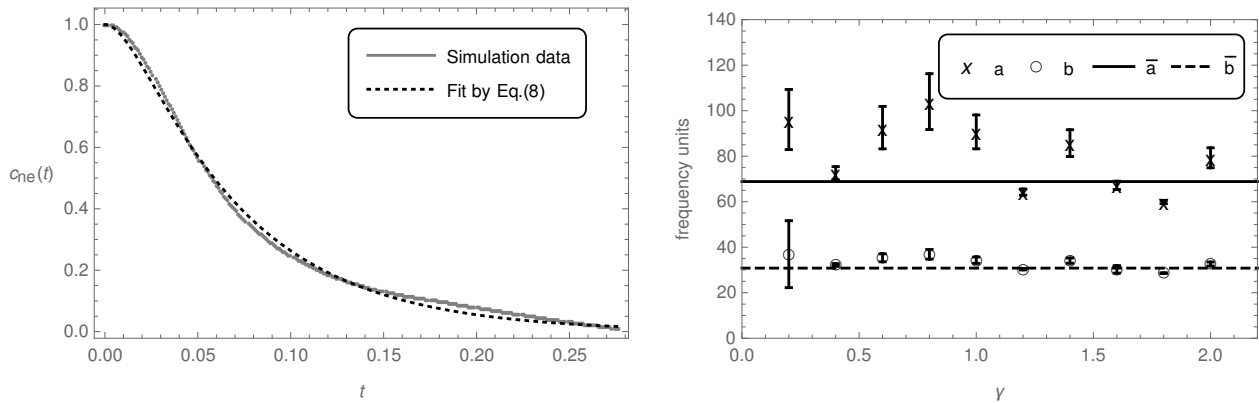


FIG. 4. Fitting Eq. (8) to the normalized autocorrelation function $c_{ne}(t)$, observed in our nonequilibrium simulations. Left panel: example of $c_{ne}(t)$ for one of our simulations at the shear rate $\gamma = 1$. Right panel: the fitting parameters a and b of Eq. (8), computed for our simulations at various shear rates; the solid horizontal lines \bar{a} and \bar{b} are, respectively, the average values of a and b , weighted by their standard deviations; error bars are given by three standard deviations.

pute κ_2 for the equilibrium fluctuations, whereas $\kappa_2(P_{xy})$ etc. are estimated separately. Finally, the variance of nonequilibrium fluctuations is greater, cf. Eq. (A12) for $B \neq 0$. Therefore, under otherwise equal conditions, Eq. (13) is subject to tighter statistical constraints, than Eq. (20).

An example of $c_{ne}(t)$, constructed for one of our nonequilibrium steady-state simulations and fitted by Eq. (8), can be found in the left panel of Fig. 4. A quite good agreement between the computational data and the analytical formula appears slightly worse, than it was in Fig. 1 for the equilibrium simulations. This is due to the larger statistical uncertainties of Eq. (20), as explained above.

The right panel of Fig. 4 presents the fitting parameters of Eq. (8) for $c_{ne}(t)$ calculated for our nonequilibrium simulations at various shear rates. There is a tendency to overestimation of a and b due to the same error bias, which was noted earlier in Fig. 3. To mitigate this effect, we compute the average values of the fitting parameters, weighted by their standard deviations:

$$\bar{a} = n_\gamma^{-1} \sum_i a(\gamma_i) / \Delta a(\gamma_i) \quad (21)$$

and similarly for \bar{b} , where n_γ^{-1} is the number of estimations $a(\gamma_i)$ with the standard deviations $\Delta a(\gamma_i)$.

Table II compares the final estimations of the parameters in our analytical model of autocorrelation function Eq. (8) for equilibrium and nonequilibrium simulations. The results support our conclusion, that a and b are independent of the shear rate. The estimations obtained from equilibrium and nonequilibrium data are very close, although the latter are subject to a larger statistical uncertainty, as was already discussed.

Although the independence of the autocorrelation parameters a and b from the external force is rather unexpected, it may be explained by the constant viscosity

coefficient. Indeed, the shear viscosity is related to a and b by several relations, cf. Eqs. (5,12, and 17). If the transport coefficient is constant in the constitutive relation Eq. (12), either there must be some peculiar relations between the constants of Eq. (3), e.g. b and B/τ due to Eqs. (5 and 12), either some of these constants must remain unaffected by the shear rate. The latter case, which was observed in our simulations, also appears the more likely of the two.

IV. CONCLUSION

In Sec. II we applied a recent extension of the Langevin equation [8], to generalize the Onsager-Machlup fluctuation theory of the second order in time for equilibrium and nonequilibrium steady states. A solution technique for this class of stochastic dynamical problems was demonstrated in Appendix A.

The analytical expression of the time autocorrelation function, Eq. (2), derived in Appendix B for the second-order fluctuation theory, correctly describes not only the exponential decay of the correlations, but also their smooth behavior at short times. Our computational study of the hydrodynamic shear flow confirmed that the generalized Onsager-Machlup theory is applicable to

TABLE II. Parameters of the autocorrelation function Eq. (8), determined from our equilibrium and nonequilibrium simulations. The nonequilibrium estimations are evaluated by the weighted averages, see Eq. (21)

	a	b
Equilibrium simulations, $c_{eq}(t)$	68.28 ± 0.76	31.93 ± 0.17
Nonequilibrium simulations, $c_{ne}(t)$	69 ± 13	30.8 ± 2.7

the current fluctuations. In particular, plugged into the Green-Kubo formula, Eq. (2) renders excellent results for the transport coefficient.

In our simulations, we found that the normalized correlation function of shear flow, specified by the deterministic part of the fluctuation dynamics, is practically independent of the external shear rate in the linear nonequilibrium regime. This can be attributed to the connection between the constant transport coefficient, shear viscosity in our case, and the parameters of Eq. (2).

Finally, we would like to remark, that a second-order time derivative introduces into the Langevin dynamics a dependence on the history of the fluctuating state variable. This provides a link with the formalism of the memory function [19, 20, Chapter 4], which is widely used, e.g. in the hydrodynamics. Therefore Eq. (2) might find further applications in this context.

ACKNOWLEDGMENTS

One of the authors, Dr. Roman Belousov, is obliged to Dr. Alexei Bazavov for stimulating discussions on operator splitting techniques for molecular dynamics simulations.

Appendix A: Statistics of the second-order fluctuation dynamics

As described in Sec. II, in order to complete the solution of Eq. (3), which was stated formally by Eqs. (6 and 7), one needs to specify the probability distribution of the following random processes $r(t)$ and $\dot{r}(t)$:

$$r(t) = \int_0^t ds \phi(t-s) \epsilon(s); \quad \dot{r}(t) = \int_0^t ds \dot{\phi}(t-s) \epsilon(s), \quad (\text{A1})$$

where $\epsilon(t)$ is given by Eq. (4).

In this appendix we will deal with this problem in a slightly more general way than in Sec. II, so that our result will be valid not only for exponential noise, proposed in [8]. In particular, our solution also applies to some variants of shot noise [6–8]. More specifically, we will treat a general stochastic process with stationary independent increments

$$R(t) = \int_0^t ds \epsilon(s), \quad (\text{A2})$$

such that its cumulant-generating function can be represented as:

$$\mathcal{C}_R(\tilde{R}, t) = t f(\tilde{R}). \quad (\text{A3})$$

Here \tilde{R} is the reciprocal dual of R , while $f(\cdot)$ is a cumulant-generating function of some random variable, which we call further an *elementary* cumulant-generating function of $R(t)$. The representation Eq. (A3) applies

to the Wiener process, the Gamma process, the Poisson process or a sum composed of these,⁵ cf. [8, Table I].

From now onwards, reciprocal duals of random variables are denoted by tilde, like we already used above \tilde{R} for the dual of R . To proceed, we will need the following lemma.

Lemma 1. *Let R and \tilde{R} be, respectively, a real random variable and its reciprocal dual with a cumulant-generating function $\mathcal{C}_R(\tilde{R})$. Then a joint cumulant-generating function of random variables $\rho_1 = c_1 R$ and $\rho_2 = c_2 R$, where c_1 and c_2 are real constants, is given by*

$$\mathcal{C}_\rho(\tilde{\rho}_1, \tilde{\rho}_2) = \mathcal{C}_R(c_1 \tilde{\rho}_1 + c_2 \tilde{\rho}_2), \quad (\text{A4})$$

where $\tilde{\rho}_1$ and $\tilde{\rho}_2$ are reciprocal duals of ρ_1 and ρ_2 , respectively.

Proof. Let us introduce an auxiliary random variable $R' = R$. Then a joint probability density of R and R' is $p(R, R') = p(R) \delta(R - R')$, where $p(R)$ is the probability density of R and $\delta(\cdot)$ is the Dirac delta-function. The joint probability measure of ρ_1 and ρ_2 is

$$p_\rho(\rho_1, \rho_2) d\rho_1 d\rho_2 = p(\rho_1/c_1, \rho_2/c_2) \frac{d\rho_1}{c_1} \frac{d\rho_2}{c_2},$$

whence we have:

$$\begin{aligned} \mathcal{C}_\rho(\tilde{\rho}_1, \tilde{\rho}_2) &= \ln \iint d\rho_1 d\rho_2 \exp(\rho_1 \tilde{\rho}_1 + \rho_2 \tilde{\rho}_2) p_\rho(\rho_1, \rho_2) \\ &= \ln \iint dR dR' \exp(c_1 R \tilde{\rho}_1 + c_2 R' \tilde{\rho}_2) p(R) \delta(R - R') \\ &= \ln \iint dR \exp[R(c_1 \tilde{\rho}_1 + c_2 \tilde{\rho}_2)] p(R) \\ &= \mathcal{C}_R(c_1 \tilde{\rho}_1 + c_2 \tilde{\rho}_2), \end{aligned} \quad (\text{A5})$$

which proves the lemma. \square

Now we express $r(t)$ and $\dot{r}(t)$ from Eq. (A1), as limits of the following discrete sums, s and \dot{s}_n , respectively, by partitioning the domain $[0, t]$ into n subintervals of length Δt so that $n\Delta t = t$:

$$\begin{aligned} S(n) &= \sum_{j=0}^{n-1} \phi(t - j\Delta t) \int_{j\Delta t}^{(j+1)\Delta t} ds \epsilon(s) \\ &= \sum_{j=0}^{n-1} \phi(t - j\Delta t) R(\Delta t) = \sum_{j=0}^{n-1} R_j \xrightarrow{n \rightarrow \infty} r(t) \end{aligned} \quad (\text{A6})$$

where we used Eq. (A2), and similarly,

$$\dot{S}(n) = \sum_{j=0}^{n-1} \dot{\phi}(t - j\Delta t) R(\Delta t) = \sum_{j=0}^{n-1} \dot{R}_j \xrightarrow{n \rightarrow \infty} \dot{r}(t). \quad (\text{A7})$$

⁵ The representation Eq. (A3) of the stationary stochastic processes, mentioned in this paper, is related to their property of *infinite divisibility* [21].

By assumption, $R(t)$ has independent stationary increments. Therefore the terms R_j in Eq. (A6) are mutually independent. The same argument also applies to \dot{R}_j in Eq. (A7). Consequently, the joint cumulant-generating function $\mathcal{C}_{S\dot{S}}(\cdot, \cdot, n)$ for S and \dot{S} equals the sum of the joint cumulant-generating functions of R_j and \dot{R}_j , $\mathcal{C}_j(\cdot, \cdot)$. By applying Lemma 1 to the latter and using the representation Eq. (A3), this yields:

$$\begin{aligned} \mathcal{C}_{S\dot{S}}(\tilde{S}, \tilde{\dot{S}}, n) &= \sum_{j=0}^{n-1} \mathcal{C}_j(\tilde{S}, \tilde{\dot{S}}) \\ &= \sum_{j=0}^{n-1} \mathcal{C}_R[\phi(t-j\Delta t)\tilde{S} + \dot{\phi}(t-j\Delta t)\tilde{\dot{S}}, \Delta t] \\ &\xrightarrow{n \rightarrow \infty} \int_0^t ds f[\phi(t-s)\tilde{r} + \dot{\phi}(t-s)\tilde{\dot{r}}] \\ &= \mathcal{C}_{r\dot{r}}(\tilde{r}, \tilde{\dot{r}}, t), \end{aligned} \quad (\text{A8})$$

which is the joint cumulant-generating function of $r(t)$ and $\dot{r}(t)$. By repeating the above derivation for the marginal distributions of $r(t)$ and $\dot{r}(t)$, one can obtain separately their cumulant-generating functions:

$$\mathcal{C}_r(\tilde{r}, t) = \int_0^t ds f[\phi(t-s)\tilde{r}] \quad (\text{A9})$$

$$\mathcal{C}_{\dot{r}}(\tilde{\dot{r}}, t) = \int_0^t ds f[\dot{\phi}(t-s)\tilde{\dot{r}}]. \quad (\text{A10})$$

The integral representations Eqs. (A8-A10) allow to compute analytically the cumulants of r and \dot{r} , once the elementary cumulant-generating function f is specified. Since in Sec. II and Appendix B we are mainly interested in the steady-state solution of Eq. (3), α_{SS} and $\dot{\alpha}_{\text{SS}}$, below

we calculate their cumulants κ_i , $i = 1..3$:

$$\begin{aligned} \kappa_1(\alpha_{\text{SS}}) &= \lim_{t \rightarrow \infty} \frac{\partial \mathcal{C}_r}{\partial r}(0, t) = \frac{f'(0)}{b^2} \\ \kappa_2(\alpha_{\text{SS}}) &= \lim_{t \rightarrow \infty} \frac{\partial^2 \mathcal{C}_r}{\partial r^2}(0, t) = \frac{f''(0)}{2ab^2} \\ \kappa_3(\alpha_{\text{SS}}) &= \lim_{t \rightarrow \infty} \frac{\partial^3 \mathcal{C}_r}{\partial r^3}(0, t) = \frac{2f^{(3)}(0)}{3b^2(2a^2 + b^2)} \\ \kappa_1(\dot{\alpha}_{\text{SS}}) &= \lim_{t \rightarrow \infty} \frac{\partial \mathcal{C}_{\dot{r}}}{\partial \dot{r}}(0, t) = 0 \\ \kappa_2(\dot{\alpha}_{\text{SS}}) &= \lim_{t \rightarrow \infty} \frac{\partial^2 \mathcal{C}_{\dot{r}}}{\partial \dot{r}^2}(0, t) = \frac{f''(0)}{2a} \\ \kappa_3(\dot{\alpha}_{\text{SS}}) &= \lim_{t \rightarrow \infty} \frac{\partial^3 \mathcal{C}_{\dot{r}}}{\partial \dot{r}^3}(0, t) = \frac{2af^{(3)}(0)}{3(2a^2 + b^2)}, \end{aligned} \quad (\text{A11})$$

where f' , f'' , $f^{(3)}$ denote the derivatives of the elementary cumulant-generating function. For the stochastic noise, defined by Eq. (4), we have

$$f(\tilde{R}) = A^2 \tilde{R}/2 - \ln(1 - B\tilde{R})/\tau,$$

which, due to Eq. (A11), renders the following cumulants of α_{SS}

$$\kappa_3(\alpha_{\text{SS}}) = \frac{4B^3}{3b^2\tau(2a^2 + b^2)}. \quad (\text{A12})$$

Appendix B: Time autocorrelation function of the second-order fluctuation dynamics

In this section we prove Eq. (11) by using the results of Appendix A. For convenience we adopt a subscript notation $\alpha_t = \alpha(t)$. Consider the joint steady-state probability function of α_0 and α_t , which can be written as:

$$p_{0,t}(\alpha_0, \alpha_t) = \int d\dot{\alpha}_0 p_t(\alpha_t|\alpha_0, \dot{\alpha}_0) p(\alpha_0, \dot{\alpha}_0), \quad (\text{B1})$$

where $p(\cdot, \cdot)$ is the joint steady-state probability density of α_{SS} and $\dot{\alpha}_{\text{SS}}$, while $p_t(\alpha_t|\alpha_0, \dot{\alpha}_0)$ is the transition probability to the state α_t , conditional on some initial state $\alpha_0, \dot{\alpha}_0$. But, due to Eq. (6), we have

$$p_t(\alpha_t|\alpha_0, \dot{\alpha}_0) = p_r[\alpha_t - \alpha_0 c(t) + \dot{\alpha}_0 \dot{c}(t)/b^2], \quad (\text{B2})$$

where $p_r(\cdot)$ is the probability density of $r(t)$ from Eq. (A1), which corresponds to the cumulant-generating function $\mathcal{C}_r(\cdot, t)$ from Eq. (A9).

By using Eqs. (B1 and B2), for the probability distribution $p_{0,t}(\cdot, \cdot)$ we obtain the following joint cumulant-generating function:

$$\begin{aligned}
\mathcal{C}_{0,t}(\alpha_0, \alpha_t) &= \ln \iint d\alpha_0 d\alpha_t \exp(\alpha_0 \tilde{\alpha}_0 + \alpha_t \tilde{\alpha}_t) p_{0,t}(\alpha_0, \alpha_t) \\
&= \ln \iiint d\dot{\alpha}_0 d\alpha_0 d\alpha_t \exp(\alpha_0 \tilde{\alpha}_0 + \alpha_t \tilde{\alpha}_t) p(\alpha_0, \dot{\alpha}_0) p_r[\alpha_t - \alpha_0 c(t) + \dot{\alpha}_0 \dot{c}(t)/b^2] \\
&= \mathcal{C}_r(\tilde{\alpha}_t, t) + \ln \iint d\dot{\alpha}_0 d\alpha_0 \exp\{\alpha_0 [\tilde{\alpha}_0 + \tilde{\alpha}_t c(t)] - \dot{\alpha}_0 \tilde{\alpha}_t \dot{c}(t)/b^2\} p(\alpha_0, \dot{\alpha}_0) \\
&= \mathcal{C}_r(\tilde{\alpha}_t, t) + \lim_{t' \rightarrow \infty} \mathcal{C}_{r\dot{r}}[\tilde{\alpha}_0 + \tilde{\alpha}_t c(t), -\tilde{\alpha}_t \dot{c}(t)/b^2, t'],
\end{aligned} \tag{B3}$$

where $\mathcal{C}_{r\dot{r}}(\cdot, \cdot, t)$ is given by Eq. (A8). The normalized autocorrelation function $c_\alpha(t)$ follows from Eqs. (A8 and B3):

$$\begin{aligned}
c_\alpha(t) &= \frac{1}{\kappa_2(\alpha_{SS})} \frac{\partial^2 \mathcal{C}_{0,t}}{\partial \alpha_t \partial \alpha_0}(0, 0) = \frac{1}{\kappa_2(\alpha_{SS})} \lim_{t' \rightarrow \infty} \frac{\partial^2 \mathcal{C}_{r\dot{r}}[\tilde{\alpha}_0 + \tilde{\alpha}_t c(t), -\tilde{\alpha}_t \dot{c}(t)/b^2, t']}{\partial \alpha_t \partial \alpha_0} \bigg|_{\substack{\alpha_0=0 \\ \alpha_t=0}} \\
&= \frac{c(t)f''(0)}{\kappa_2(\alpha_{SS})} \lim_{t' \rightarrow \infty} \left[\int_0^{t'} ds \phi(t' - s)^2 \right] + \frac{\dot{c}(t)f''(0)}{b^2 \kappa_2(\alpha_{SS})} \lim_{t' \rightarrow \infty} \left[\int_0^{t'} ds \phi(t' - s) \dot{\phi}(t' - s) \right] = c(t),
\end{aligned} \tag{B4}$$

which concludes our proof of Eq. (11).

Appendix C: Details of the computational model

In our molecular dynamics simulations, we integrated numerically equations of motion in $D = 3$ dimensions for a system of $N = 10000$ particles, which were interacting through the Weeks-Chandler-Anderson potential [15]:

$$U_{\text{WCA}}(r) = \begin{cases} 4\epsilon \left[\left(\frac{\sigma}{r} \right)^{12} - \left(\frac{\sigma}{r} \right)^6 \right], & \text{if } r < 2^{1/6} \sigma \\ 0, & \text{if } r \geq 2^{1/6} \sigma \end{cases},$$

where r is the interparticle distance, ϵ and σ are constants of the potential energy and its range, respectively.

The system was subject to moving periodic boundary conditions, which impose a constant shear rate γ [16, Chapter 6], and coupled to the Nosé-Hoover (NH) thermostat [22, Chapter 6] of the relaxation time constant θ . The resulting thermostatted SLLOD [16, Chapter 6] equations of motion read:

$$\begin{aligned}
\dot{\mathbf{q}}_i &= \mathbf{p}_i/m + \gamma q_{iy} \mathbf{X} \\
\dot{\mathbf{p}}_i &= \mathbf{F}_i(\mathbf{q}_i) - \gamma p_{iy} \mathbf{X} - \zeta \mathbf{p}_i \\
\dot{\zeta} &= \theta^{-2} \sum_{i=1}^N \left(\frac{\mathbf{p}_i^2}{m D N k_B T} - 1 \right).
\end{aligned} \tag{C1}$$

Here \mathbf{X} is a unit vector along the Cartesian coordinate axis X and \mathbf{q}_i is the position of i -th particle (q_{iy} being its Y -coordinate); all particles have equal mass m ; \mathbf{p}_i is the *peculiar* linear momentum of the i -th particle (p_{iy} being its Y -component); \mathbf{F}_i is the force on the i -th particle due to the interactions with all the other particles; ζ is the coupling to the NH reservoir at temperature T , while k_B is the Boltzmann constant. The pressure tensor

components are calculated by the following formula:

$$P_{xy} = V^{-1} \sum_{i=1}^N (p_{ix} p_{iy} / m + F_{ix} q_{iy}),$$

and similarly for P_{yz} and P_{zy} .

The results of Sec. III are reported in simulation units, reduced by the energy constant ϵ , the length constant σ , the mass constant m and the time constant θ . Invariant parameters of our computational experiments were the temperature of the NH thermostat $k_B T = 1$ and the number density 0.8.

The numerical integration of Eq. (C1) was performed with a time step $\Delta t = 10^{-3}$ by using an optimized version of the symplectic operator-splitting method, proposed in Ref. [23]. In more detail, we consider an evolution operator, acting on the extended phase space of points $\mathbf{\Gamma} = (\mathbf{q}_{1..N}, \mathbf{p}_{1..N}, \zeta)$, so that

$$\mathbf{\Gamma}(t) = \exp(i\mathcal{L}t) \mathbf{\Gamma}(0),$$

where $i\mathcal{L} = \dot{\mathbf{\Gamma}} \cdot \nabla_{\mathbf{\Gamma}}$ is the Liouville operator for Eq. (C1). The Liouvillian can be split by using the following operatorial sum:

$$\begin{aligned}
\mathcal{L} &= \mathcal{L}_{p\gamma} + \mathcal{L}_p + \mathcal{L}_{p\zeta} + \mathcal{L}_{q\gamma} + \mathcal{L}_{q\zeta} \\
i\mathcal{L}_{q\zeta} &= \frac{\mathbf{p}}{m} \cdot \partial_{\mathbf{q}} + \dot{\zeta} \partial_{\zeta} \\
i\mathcal{L}_{q\gamma} &= \gamma \mathbf{q}_y \cdot \frac{\partial}{\partial \mathbf{q}_x} \\
i\mathcal{L}_{p\zeta} &= -\zeta \mathbf{p} \cdot \partial_{\mathbf{p}} \\
i\mathcal{L}_p &= \mathbf{F}(\mathbf{q}) \cdot \partial_{\mathbf{p}} \\
i\mathcal{L}_{p\gamma} &= -\gamma \mathbf{p}_y \cdot \frac{\partial}{\partial \mathbf{p}_x},
\end{aligned} \tag{C2}$$

where the operators $\partial_{\mathbf{q}}$, $\partial_{\mathbf{p}}$ etc. act on the respective subspaces of positions \mathbf{q} , momenta \mathbf{p} etc. in $\mathbf{\Gamma}$. The evolution operator is then approximated by

$$\begin{aligned} \exp[i\mathcal{L}t + O(t^2)] &= \prod_{j=1}^{t/\Delta t} \exp\left(\frac{i\mathcal{L}_{p\gamma}\Delta t}{2}\right) \exp\left(\frac{i\mathcal{L}_p\Delta t}{2}\right) \exp\left(\frac{i\mathcal{L}_{p\zeta}\Delta t}{2}\right) \exp\left(\frac{i\mathcal{L}_{q\gamma}\Delta t}{2}\right) \times \\ &\times \exp(i\mathcal{L}_{q\zeta}\Delta t) \exp\left(\frac{i\mathcal{L}_{q\gamma}\Delta t}{2}\right) \exp\left(\frac{i\mathcal{L}_{p\zeta}\Delta t}{2}\right) \exp\left(\frac{i\mathcal{L}_{p\gamma}\Delta t}{2}\right) \exp\left(\frac{i\mathcal{L}_p\Delta t}{2}\right). \end{aligned} \quad (\text{C3})$$

The decomposition of the evolution operator in Eq. (C3) determines the sequence of steps in our symplectic integrator, as described in Refs [22–24, Appendix E].

Before collecting simulation data, the initially generated phase space configurations were evolved for a time

interval of 10^5 reduced units. Then, in order to calculate the autocorrelation functions of interest, we measured the pressure tensor components at 10^5 consecutive integration steps.

-
- [1] L. Onsager and S. Machlup, Phys. Rev. **91**, 1505 (1953).
 - [2] S. Machlup and L. Onsager, Phys. Rev. **91**, 1512 (1953).
 - [3] L. Landau, E. Lifshitz, and L. Pitaevskii, *Statistical Physics*, 3rd ed. (Pergamon Press, Oxford, New York, 1980).
 - [4] P. Attard, *Non-Equilibrium Thermodynamics and Statistical Mechanics* (Oxford University Press, Oxford, 2012).
 - [5] K. Kanazawa, T. G. Sano, T. Sagawa, and H. Hayakawa, Phys. Rev. Lett. **114**, 090601 (2015).
 - [6] K. Kanazawa, T. G. Sano, T. Sagawa, and H. Hayakawa, Journal of Statistical Physics **160**, 1294 (2015).
 - [7] W. A. M. Morgado and S. M. D. Queirós, Phys. Rev. E **93**, 012121 (2016).
 - [8] R. Belousov, E. G. D. Cohen, and L. Rondoni, Phys. Rev. E **94**, 032127 (2016).
 - [9] R. Belousov, E. G. D. Cohen, C.-S. Wong, J. A. Goree, and Y. Feng, Phys. Rev. E **93**, 042125 (2016).
 - [10] S. Bonella, G. Ciccotti, and L. Rondoni, EPL (Europhysics Letters) **108**, 60004 (2014).
 - [11] S. Dal Cengio and L. Rondoni, Symmetry **8**, 73 (2016).
 - [12] L. Onsager, Phys. Rev. **37**, 405 (1931).
 - [13] J. Haile, *Molecular dynamics simulation: elementary methods* (Wiley, New York, 1992).
 - [14] S. Chandrasekhar, Rev. Mod. Phys. **15**, 1 (1943).
 - [15] J. D. Weeks, D. Chandler, and H. C. Andersen, **54**, 5237 (1971).
 - [16] D. J. Evans and G. P. Morriss, *Statistical Mechanics of Nonequilibrium Liquids*, 2nd ed. (ANUE Press, Canberra, 2007).
 - [17] A. N. Lagar’kov and V. M. Sergeev, Soviet Physics Uspekhi **21**, 566 (1978).
 - [18] J. Kenney and E. Keeping, *Mathematics of Statistics*, 2nd ed., Vol. 2 (D. Van Nostrand Company, New York, 1951).
 - [19] P. Adamo, R. Belousov, and L. Rondoni, “Fluctuation-dissipation and fluctuation relations: From equilibrium to nonequilibrium and back,” in *Large Deviations in Physics: The Legacy of the Law of Large Numbers*, edited by A. Vulpiani, F. Cecconi, M. Cencini, A. Puglisi, and D. Vergni (Springer Berlin Heidelberg, Berlin, Heidelberg, 2014) pp. 93–133.
 - [20] J. P. Boon and S. Yip, *Molecular hydrodynamics* (McGraw-Hill, New York, 1980).
 - [21] F. Steutel, J. Kent, L. Bondesson, and O. Barndorff-Nielsen, Scandinavian Journal of Statistics **6**, 57 (1979).
 - [22] D. Frenkel and B. Smit, *Understanding of Molecular Dynamics Simulations: From Algorithms to Applications* (Academic Press, San Diego, 2002).
 - [23] G. J. Martyna, M. E. Tuckerman, D. J. Tobias, and M. L. Klein, Molecular Physics **87**, 1117 (1996), <http://dx.doi.org/10.1080/00268979600100761>.
 - [24] G. J. Martyna and M. E. Tuckerman, The Journal of Chemical Physics **102** (1995).